



N OVA
NOVA SCHOOL OF
SCIENCE & TECHNOLOGY

DEPARTMENT OF
MATERIALS SCIENCE

RICARDO MANUEL MONTEIRO CALADO
BSc in Micro and Nanotechnology Engineering

ADDITIVE MANUFACTURING OF
RESETTABLE-DEFORMATION BI-STABLE
LATTICES BASED ON A COMPLIANT
MECHANISM

MASTER IN MICRO AND NANOTECHNOLOGY ENGINEERING
NOVA University Lisbon
September, 2022



ADDITIVE MANUFACTURING OF RESETTABLE-DEFORMATION BI-STABLE LATTICES BASED ON A COMPLIANT MECHANISM

RICARDO MANUEL MONTEIRO CALADO

BSc in Micro and Nanotechnology Engineering

Adviser: Alexandre José da Costa Velhinho
Assistant Professor, NOVA University Lisbon

Co-advisers: João Paulo Miranda Ribeiro Borges
Associate Professor w/ Habilitation, NOVA University Lisbon

Examination Committee:

Chair: Hugo Manuel Brito Águas,
Associate Professor, FCT-NOVA

Rapporteur: Bruno Alexandre Rodrigues Simões Soares,
Assistant Professor, FCT-NOVA

Adviser: Alexandre José da Costa Velhinho,
Assistant Professor, FCT-NOVA

Additive Manufacturing of Resettable-Deformation Bi-Stable Lattices Based on a Compliant Mechanism

Copyright © Ricardo Manuel Monteiro Calado, NOVA School of Science and Technology, NOVA University Lisbon. The NOVA School of Science and Technology and the NOVA University Lisbon have the right, perpetual and without geographical boundaries, to file and publish this dissertation through printed copies reproduced on paper or on digital form, or by any other means known or that may be invented, and to disseminate through scientific repositories and admit its copying and distribution for non-commercial, educational or research purposes, as long as credit is given to the author and editor.

“If I have seen further, it is by standing on the
shoulders of giants.”

Isaac Newton.

ACKNOWLEDGMENTS

First of all, I would like to thank my supervisors, Professor Alexandre Velhinho and Professor João Paulo Borges, for all their availability, patience, and guidance throughout a very interesting and challenging work, being very grateful for the opportunity that was given to me.

I would also like to thank the entire team at DCM and CENIMAT, as well as all Professors at the Department of Material Sciences, for their indispensable support throughout my academic route. In particular, I would like to thank João Cardoso for all the help and support provided throughout the lab experiments carried out to write this thesis. I am very grateful to have been allowed to use the lab equipment to fabricate the structures and making the fundamental mechanical characterization to draw the corresponding conclusions about their usefulness.

A special thanks to my family, for all the love, sacrifice and unconditional support and patience indispensable for my growth; I also thank them for transmitting precious and eternal values to me.

Last but not the least, I am very grateful for all the support and encouragement given to me by Professor António Abreu.

ABSTRACT

Metamaterials allow for the possibility to design and fabricate new materials with enhanced mechanical properties, through the use of additive manufacturing. There are some certain materials' structures that exhibit excellent properties to withstand externally applied forces. One example of this type of structure is a bi-stable switching mechanism which can regain its original position, after being submitted to a compressive force. This kind of structure should be flexible and strong since it needs to undergo a certain deflection. Another important aspect that was addressed in this work is the structure's geometry, because of the effect that it has on flexibility. Therefore, this thesis will focus on the proper study, design, 3D printing, and mechanical characterization of a novel unitary compliant bi-stable structure, and its use to build two larger cellular compliant bi-stable structures, a four-cell and a multicell structure, using the unitary one as a building block. All structures were designed in the CAD software Fusion 360 and fabricated with Polylactic Acid filament using the Fused Filament Fabrication process. The fabricated structures were submitted to compressive tests, from where Force vs. Displacement plots were obtained. These results proved that the multicell structure was the stiffest, since it required higher compressive force to perform its function, when compared to the other two structures. The conducted tests were important to check the behavior of each structure while being compressed, where both structures that had more than one cell showed a layered switching behavior. Also, the tests were important to check if the position recovery of the structures was possible to achieve, which was observed in all of them. After the compressive tests, all structures were also submitted to repetitive solicitation tests, to study their repeatability behavior. These results envisage the successful application of these mechanisms towards their implementation in microelectromechanical systems.

Keywords: Mechanical Metamaterials, Bi-Stable Metamaterials, Additive Manufacturing, 3D Printing.

RESUMO

Os metamateriais permitem fabricar novos materiais com propriedades mecânicas aprimoradas, através do uso de manufatura aditiva. Existem algumas estruturas de determinados materiais que apresentam excelentes propriedades para resistir às forças externas aplicadas sobre eles. Um exemplo deste tipo de estrutura é um mecanismo complacente biestável que pode recuperar a sua posição original, após ser submetido a uma força de compressão. Este tipo de estrutura precisa de ser flexível e forte, porque é projetado para sofrer uma certa deflexão. Outro aspeto importante que foi abordado neste trabalho é a geometria da estrutura, devido ao efeito que esta tem na flexibilidade. Portanto, esta dissertação concentrar-se-á no estudo adequado, desenho, impressão 3D e caracterização mecânica de uma nova estrutura complacente biestável unitária, e o seu uso para construir duas estruturas celulares complacentes biestáveis, uma de quatro células e outra multicelular, usando a estrutura unitária como bloco de construção. Todas as estruturas foram desenhadas no software de CAD Fusion 360 e fabricadas com filamento de Ácido Poliláctico usando o processo de Fabricação com Filamento Fundido. As estruturas fabricadas foram submetidas a ensaios de compressão, de onde foram obtidos gráficos de Força vs. Deslocamento. Estes resultados comprovaram que a estrutura multicelular era a mais rígida, porque necessitou de uma maior força compressiva para desempenhar a sua função. Os testes realizados foram importantes para analisar o comportamento de cada estrutura durante a compressão, onde ambas as estruturas multicelulares apresentaram um comportamento de transição camada a camada. Além disso, os testes foram também importantes para verificar se a recuperação da posição das estruturas era possível, o que foi observado para todas. Após os ensaios de compressão, todas as estruturas foram submetidas a ensaios de solitação repetitiva, para estudar o seu comportamento de repetibilidade. Estes resultados vislumbram o sucesso da implementação destes mecanismos em sistemas microelectromecânicos.

Palavras chave: Metamateriais Mecânicos, Metamateriais Biestáveis, Manufatura Aditiva, Impressão 3D.

CONTENTS

LIST OF FIGURES	XVII
ACRONYMS	XIX
1 INTRODUCTION	1
1.1 Motivation and Objectives	4
2 LITERATURE REVIEW	5
2.1 Compliance	5
2.2 Additive Manufacturing.....	6
2.2.1 Mechanical Metamaterials Fabrication	6
2.2.2 Bi-Stable Metamaterials Fabrication	9
2.2.3 Fused Filament Fabrication	10
2.2.4 Polylactic Acid	10
3 METHODOLOGY	12
3.1 Compliant Mechanism Structure Design and Testing	12
4 CASE STUDIES	15
4.1 Single Cell Switching Mechanism	18
4.2 Four-Cell Switching Mechanism.....	19
4.3 Multicell Switching Mechanism	22
5 CONCLUSIONS AND FUTURE PERSPECTIVES.....	25
BIBLIOGRAPHY	27

LIST OF FIGURES

Figure 1.1 — Structure with actuated mass and flexible actuators (adapted from [1]) -----	1
Figure 1.2 — Bending- (a) and stretching-dominated (b) behavior in cellular materials (adapted from [3]) -----	3
Figure 1.3 — Energy trade schematic representation of a compliant mechanism (adapted from [13]) -	3
Figure 2.1 — Examples of compliance in nature: a spine, bee wigs, elephant trunks, blooming flowers, mosquito, seaweed, and eels -----	5
Figure 3.1 — Two four-cell TPU structures -----	13
Figure 3.2 — Compression essay on a four-cell switching mechanism -----	13
Figure 4.1 — Sketch of the single cell switching mechanism (Fusion 360) -----	15
Figure 4.2 — Single cell switching mechanism (Fusion 360) -----	15
Figure 4.3 — 3D printing overview of the single cell mechanism (Fusion 360) -----	16
Figure 4.4 — Four-cell switching mechanism (Fusion 360) -----	16
Figure 4.5 — Multicell switching mechanism (Fusion 360) -----	16
Figure 4.6 — Established angle between the arms and the frame (Fusion 360) -----	17
Figure 4.7 — Experimental compression test results done on Cherry <i>et al.</i> 's switching mechanism [51] -----	18
Figure 4.8 — Single cell switching mechanism (after printing) -----	18
Figure 4.9 — Compression curve of the single cell switching mechanism -----	19
Figure 4.10 — Sketch of the four-cell switching mechanism (Fusion 360) -----	20
Figure 4.11 — 3D printing overview of the four-cell switching mechanism (Cura) -----	20
Figure 4.12 — Four-cell switching mechanism (after printing) -----	21
Figure 4.13 — Compression curve of the four-cell switching mechanism -----	22
Figure 4.14 — 3D printing overview of the multicell switching mechanism (Cura) -----	22
Figure 4.15 — Multicell switching mechanism (after printing) -----	23
Figure 4.16 — Compression curve of the multicell switching mechanism -----	23

ACRONYMS

3D	Three-dimensional
ALD	Atomic Layer Deposition
AM	Additive Manufacturing
CAD	Computer-Aided Design
DLW	Direct Laser Writing
FDM	Fused Deposition Modeling
FFF	Fused Filament Fabrication
FIB	Focused Ion Beam
MEMS	Microelectromechanical Systems
MPL	Multi Photon Lithography
MPP	Multi-Photon Polymerization
MSL	Micro Stereolithography
PET	Polyethylene Terephthalate
PLA	Polylactic Acid
SEBM	Selective Electron Beam Melting
SLM	Selective Laser Melting
SLS	Selective Laser Sintering
SPPW	Self-Propagating Photopolymer Waveguide
TPU	Thermoplastic Polyurethane

INTRODUCTION

The last decades' technological boost has been inducing the development of new materials with enhanced properties. A new class of materials called metamaterials, which are man-made material structures aiming to obtain properties that surpass those of the ingredient materials, has the potential to address some gaps in the materials engineering world by exhibiting new properties that are not found in nature. For instance, new metamaterials have been developed based on structures composed by an actuated mass connected to a set of flexible actuators, which can be used as systems that can store digital data without the need to use electricity, through Boolean computations based on mechanical forces and displacements, as depicted in Figure 1.1 [1].

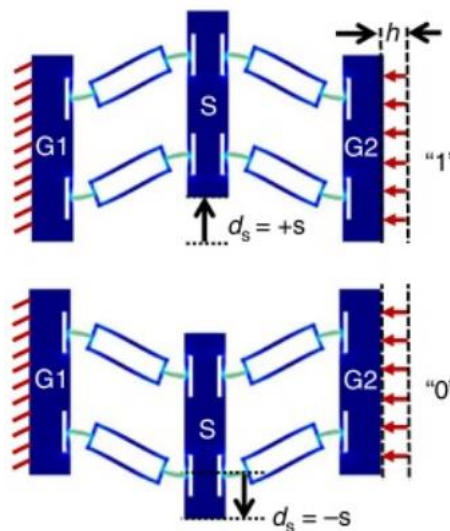


Figure 1.1 — Compliant structure with actuated mass and flexible actuators (adapted from [1]).

The metamaterials are generally designed based on periodic structures, aiming to obtain special properties that are hardly found in nature, such as high thermic insulation [2], specific stiffness higher than the observed in other well-known materials [3], negative stiffness [4], negative Poisson's ratio, being called as auxetic metamaterials [5], as well as the propagation prevention of elastic waves, hence

they may be applied in the development of frequency filters, as vibration and sound devices [6], or waveguides [7].

Recently, a higher complexity of metamaterials has been observed due to improvements in simulation computational platforms and in design tools based on machine learning techniques [8]. Therefore, the common subtractive manufacturing processes are no longer suitable to cope with the increasing geometric complexity of metamaterial structures, namely when features at a micro or nanoscale are under concern [8]. Hence, to overcome the corresponding challenges, the research community has been exploring the use of additive manufacturing techniques or three-dimensional printing processes to obtain complex geometries that otherwise would be unachievable [8]. For instance, through nanoscale additive manufacturing processes, materials and devices can be envisaged, having higher value in fields such as harvesting and energy storage, optoelectronics, electronics, biochemical sensors, among others [8].

Depending on the design, metamaterials can manifest a number of compliant directions while having high stiffness in all other directions. Therefore, some metamaterials can be built based on a compliant mechanism (CM), using the motion obtained from elastic deformations of its members to perform certain tasks. Also, these mechanisms' elastic deformation depends upon the applications they are designed for [9]. Nowadays, there are structures that exhibit excellent properties to withstand externally applied forces. One example of this type of structure is a bi-stable switching mechanism that can regain its original form after being submitted to a compressive force. This kind of structure needs to be flexible and strong since it needs to undergo a certain deflection. When talking about different materials, we need to consider their different stiffness, or Young's modulus. So, with the latter explanation in mind, the chosen material for the design of a CM would preferably need to have high strength and a low Young's modulus. Another important aspect that needs to be taken into consideration is the geometry of the structure, because of the effect that shape and size have on flexibility. Depending on certain characteristics like height, width, or orientation, different pieces of the same CM can show different behaviors after compression [10].

To achieve the desired properties of the mechanical structure, there needs to exist a good balance between the architecture and the composition [11]. Since the structure has the ability to change its shape by switching between two alternate states, some aspects like stiffness and bendability need to be addressed. Regarding this situation, the stiffness of a CM can be modified through the implementation of specific cellular arrays in the flexible parts of the system depending on the stiffness objective (increasing or reducing the stiffness). When stiffness maximization is the objective, a stretch-dominated lattice and closed cell structures are preferred. On the other hand, if flexibility is the goal, a bending-dominated auxetic and zero-Poisson's ration honeycombs are the most commonly used, as portrayed in Figure 1.2.

From what has been explained, the impact that the design has on the success of a project is clear. The first step towards the design of a CM is to establish a functional design. In this way, the desired output motion can be obtained since an input force is applied [12]. After designing a CM, it can be produced through 3D printing technology, and afterwards, a mechanical characterization of the structure should be done by conducting compression tests and simulations. This last step is very important to

determine how the material works under stress, revealing the energy absorption behavior of the structure, and how it functions in terms of repeatability and mechanical performance deterioration (fatigue testing).

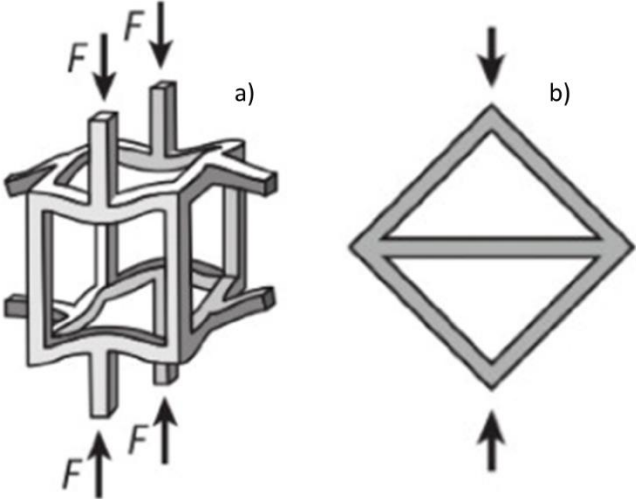


Figure 1.2 — Bending (a) and stretching-dominated (b) behavior in cellular materials (adapted from [3]).

A uniaxial tensile test (compression test) should be conducted to see if the structure is able to perform its mechanical function of switching between one position to the other. It is expected to observe this switching behavior of the structure while applying a certain compressive tension as depicted in Figure 1.3, and after that, the structure should also be able to regain its original form, meaning it does not suffer permanent deformation.

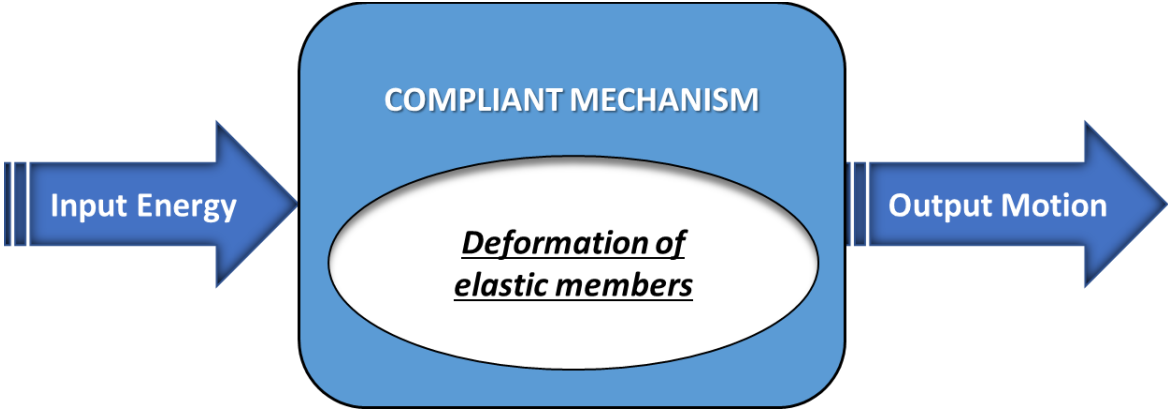


Figure 1.3 — Energy trade schematic representation of a CM (adapted from [13]).

The state-of-art concerned with additive manufacturing technologies and their relationship with the metamaterials’ fabrication, with a special focus on mechanical metamaterials, will be presented in chapter 2; aiming to guide the reader towards the main objective of this thesis, chapter 3 addresses the methodology followed to carry out the corresponding studies; hence, considering three case studies,

chapter 4 presents the obtained results and provides the respective analysis; finally, concluding remarks and future research perspectives are addressed in chapter 5.

1.1 Motivation and Objectives

As can be envisaged from what is mentioned above, metamaterials can be seen as a new class of functional materials, designed, and manufactured based on specific patterns or structures, allowing their interaction with the environment in ways not previously observed in nature. Thus, generally the properties and capabilities that characterize the metamaterials are not possible to obtain using conventional materials or even using chemical fabrication technologies. Therefore, the studies carried out underlying the writing of this thesis were motivated by the development of structures capable of implementing Boolean computing, based on mechanical forces and displacements without using electricity.

The main objective of this work, which is addressed in the following sections, is to design and fabricate a resettable metamaterial structure, with the ability to recover its initial position, after external mechanical forces are applied to it. Then, the first goal to be achieved was the development of a compliant unitary bi-stable structure composed by an actuated mass connected to a set of flexible actuators. This actuated mass should be able to switch between two stable positions due to the effect of the actuators, and this effect is of fundamental importance when talking about position recovery and repeatability. Considering the above mentioned unitary bi-stable structure, two more complex structures with bi-stable mechanisms connected to each other were designed and manufactured, aiming for the implementation of more complex Boolean functions.

This new approach considers the principles behind additive manufacturing and how one can benefit from them. The greater advantage of this type of structure is the capability of performing mechanical interactions with its surrounding, being able to process and store digital data without the need for electricity consumption. Such an approach is characterized by several advantages when compared with devices based on semiconductor electronics. It is worth emphasizing the capability to process, and storage data, based on displacements and mechanical forces applied to the devices. Furthermore, the devices development has a wide range of applications, including the ability to cope with hazardous working conditions and lower the maintenance operations. Therefore, this study aims for the development of a structure to evaluate its robustness according to the characteristics mentioned above.

Also, the work underlying this thesis led to the writing of a paper with the title “Compliant Bi-Stable Metamaterials Fabrication”, co-authored by J. O. Cardoso, J. P. Borges and A. Velhinho, which will be published by Springer and was presented by myself at the International Conference on Design for 3D Printing, Singapore, on the 22nd of September 2022.

LITERATURE REVIEW

This section aims to address the state-of-art concerned with the design and fabrication of compliant metamaterials framing the work developed and presented in the following sections.

2.1 Compliance

The first question that may arise when talking about a CM is about its definition. If something bends to perform a certain task, then it is compliant. If the flexibility that allows it to bend also helps it to perform the intended task, then it is also compliant [13].

The basic example to explain what a CM is comes from nature. Most of the moving things in nature are very flexible instead of stiff, and the motion comes from bending the flexible parts. For example, if one thinks about its heart, it is an amazing CM. Also, if one thinks about bee wings, elephant trunks, eels, seaweed, spines, and flowers, all of them are compliant, as portrayed in Figure 2.1.

Traditionally when designers need to design a machine that moves, they commonly use very stiff or rigid parts that are connected with hinges, but with CMs, the integration into fewer parts leads to compelling advantages. Firstly, this will allow to have fewer components to stock and also for the possibility of simplified manufacturing, where the low weight of CMs can be useful for weight-sensitive applications. Also, the elimination of need for lubrication at joints is a useful performance improvement. Another category of advantages lies in the ability to miniaturize CMs, such as in microelectromechanical systems (MEMS) [13].



Figure 2.1 — Examples of compliance in nature: a spine, bee wings, elephant trunks, blooming flowers, mosquito, seaweed, and eels.

2.2 Additive Manufacturing

Additive manufacturing (AM), often also referred to as three-dimensional (3D) printing, is the technological approach to build three dimensional objects, such as CMs, in a layer-by-layer basis. The AM process starts from a Computer-Aided Design (CAD) software sending a digital version of the object to a 3D printer, after being duly sliced into several layers recurring to the appropriate software for each type of 3D printer. This is the technology used for the manufacture of the CMs described in the chapters ahead.

3D printing allows for production of complex-shaped parts. 3D printed components used as energy absorption structures have recently become a very active research topic because of the high flexibility of the manufacturing process, which allows for a better control of the desired properties. This approach could be suitable to fabricate metamaterials with nested features and with increased structural complexity [10].

Currently, 3D printing is becoming more and more popular, one example being its usage in several laboratories to produce lab equipment or parts and joints, some limitations notwithstanding, such as long fabrication times, limitations on materials combination, and control over fabricated parts microstructure and functionality [14].

Considering the last decade, one can observe significant enhancements in the technology underlying the AM processes, namely as far as resolution and material availability are concerned. Hence, in more recent years AM has been used in the field of materials engineering to design and produce structures with a high degree of complexity that could not be obtain by using conventional manufacturing approaches based on replicative or subtractive technologies [14].

The improvements mentioned above concerned with the current AM capabilities have been attracting researchers working on metamaterials development and, hence, they are using this technological process to develop and produce the new generations of metamaterials. Such an approach allows for the development and production of free-standing complex 3D geometries, with a low cost associated with the manufacturing process and with an enhanced design process. Therefore, this approach allows the fabrication of metamaterials consisting of complex structures and with specific mechanical, acoustic and/or optical properties.

Awareness is due to the fact that when one wants to obtain metamaterials with specific electromagnetic and/or mechanical properties there are various AM approaches that could be used to produce them.

2.2.1 Mechanical Metamaterials Fabrication

When specific mechanical properties are needed, they could be accomplished by designing a mechanical metamaterial with a particular geometry, while the composition is less determinant to satisfy pre-defined mechanical properties [15, 16, 17].

AM technologies are able to cope with the fabrication of 3D structures with high complexity, directly from a file generated by a CAD software and, hence, it is easy to tune the mechanical properties

by adjusting the individually designed unit cells. Thus, they are the suitable technologies to fabricate mechanical metamaterials, potentially with low costs associated. Considering the types of mechanical metamaterials that are more used, below will be addressed the corresponding AM technologies that could be used to fabricate them.

Based on the literature review, Vat Polymerization technologies have been used to fabricate mechanical metamaterials with auxetic and pentamode structures [18, 19]. Under this type of technologies there are several pointed out studies where the mechanical metamaterials are fabricated using the multi-photon polymerization (MPP) technique [20].

The quite constraint building volume of the MPP technique, is one of its drawbacks. To overcome the mentioned issue, it has been proposed the division of the object to be fabricated into several small areas and, thus, larger structures could be fabricated through consecutive attempts. There are commercially available MPP devices that have a piezoelectric fabrication stage where each part is stitched with the other ones. Furthermore, mechanical metamaterials with pentamode structures have been produced through the dip-in-mode based on polymer microstructures [21].

The AM approaches based on Vat Polymerization have also been used to produce mechanical metamaterials characterized by functionalities that are different from the extremal materials. For instance, it was reported the design and fabrication of a mechanical metamaterial that twists when compressed [22], being produced by using a 3D micro printing laser.

It has also been pointed out the fabrication of mechanical metamaterials where the aim is to achieve a material with a pre-defined adjustable negative thermal expansion rate, produced through multimaterial projection based on Micro Stereolithography (MSL) [23].

A promising approach to fabricate mechanical metamaterials with the aim to develop real-life applications has been pointed out, which is a Vat Polymerization technique based on a self-propagation photopolymer waveguide methodology. This fabrication approach has been presented as having potential to be used in mass-manufacturing of large-scale micro-lattice structures without interfering in the lattice symmetry and diameter [24, 25].

According to the state-of-art, the AM technologies are not yet able to cope with the fabrication of ceramic and/or metal nanolattices with high resolution [26]. However, few hybrid fabrication approaches have been pointed out with the aim to deal with the mentioned limitation, which are based on the fabrication of a polymer lattice through a Vat Polymerization approach, at a first stage. At a second stage, the polymer lattice is processed to obtain the metal/ceramic lattices. It has also been reported the use of the above-mentioned self-propagation photopolymer waveguide methodology to produce polymer micro-lattices [27] and, afterwards, through the polymer micro-lattices pyrolysis, micro-lattice structures of glassy carbon were produced.

Self-Propagating Photopolymer Waveguide (SPPW), which is a process to fabricate ordered, open cell, interconnected, 3D polymeric lattice structures with microscale features, was adopted to produce a base polymer lattice, from which, ultralight metallic micro-lattices were fabricated, consisting of hollow tube strut elements [24, 28, 29].

By using Direct Laser Writing (DLW), which is a tool to achieve high accuracy structuring that has been put on the map as an emerging technology for scaffold 3D printing, metal-polymer composite micro-lattices by electroless plating of NiB on polymer scaffolds have been fabricated [30]. Furthermore, by applying the same technique to polymer micro-lattices, electroplating on the lattice pattern and polymer removal, it has been produced ultra-strong copper micro-lattices [31].

Fabrication techniques based on Vat Polymerization methodologies have been used to produce recoverable ceramic nanolattices [24, 32, 33]. The method that has been applied to the ceramic nanolattices production, includes a polymer scaffold 3D printing using the DLW approach, a thin alumina film deposition on the polymer scaffold through Atomic Layer Deposition (ALD), removing the outermost wall of the coated nanostructure using focused ion beam (FIB) milling, followed by the internal polymer etching. Similarly, hollow tube ceramic (alumina) micro-lattices were fabricated using MSL, ALD and thermal decomposition [23].

It is worth mentioning that hierarchical hollow tube metamaterials have been produced through hybrid fabrication techniques based on Vat Polymerization methodologies. Thus, hierarchical nanolattices in the polymer, polymer-ceramic composite, and ceramic (alumina) have been produced using the following techniques: DLW, ALD and polymer etching [34].

The Selective Laser Melting (SLM) approach has demonstrated to have high potential to be used in the production of metallic lattice structures, such as the development of automotive parts and biomedical devices based on meta-biomaterials.

The Selective Electron Beam Melting (SEBM) process has been used to produce auxetic lattice structures based on titanium alloys. This approach has demonstrated high potential to produce analytically optimized structures that traditionally will be non-manufacturable [35].

Additionally, the PolyJet printing approach has been considered a very suitable technique to produce metamaterial structures, to be applied in a variety of knowledge domains, such as control of vibrations, energy absorption and electronic devices. This technique has also been used to produce multimerial auxetic structures, which exhibit properties that are distinctive from the ones characterizing the single material auxetic metamaterials. Several examples have been reported where this technique is used to produce, for instance, soft robots' parts based on auxetic metamaterials, which are characterized for having a positive Poisson's ratio [36]. Combining methodologies to optimize the structures topologies with 3D printing has demonstrated that structures with a tuned Poisson's ratio can be produced, which can cope with high deformation ranges [37].

On the other hand, Selective Laser Sintering (SLS) technology has been reported as a suitable approach to produce macroscopic auxetic materials, as for instance based on polymers and characterized by a negative Poisson's ratio [38], between other applications reported in the literature.

Other studies have been reported where the fabrication of metamaterials is performed using the fused filament fabrication (FFF) technique, as for instance the production of rhombohedral and hexagonal unit-cells with layers thickness of 0.2 mm, where the material used is soft Polylactic Acid (PLA) [39].

2.2.2 Bi-Stable Metamaterials Fabrication

A particular type of metamaterials is drawing increased attention from the research community, namely the ones that are able to cope with mechanical transformations between two stable states. Such metamaterials are usually fabricated through the FFF technique, being the most commonly used approach to their production, which will be briefly described in a subsection below.

It has been observed that when stress is applied to a nylon-based material, an oscillation behavior between two states could be registered [40], exhibiting a clear non-linear behavior in opposite to many other mechanical materials characterized by quasi linear dynamic behaviors. Many field applications can be envisaged for such materials, namely in the field of vibration and damping.

Other studies have been pointed out where the aim is to design and fabricate metamaterials characterized by multiple bi-stable cells [41]. Those metamaterials were obtained based on a structure fabricated with a mix of multiple resins, allowing for the desired mechanical properties tuning.

A more recent work concluded that the bi-stability could be extended and by this way a multiple states behavior could be observed [42]. The metamaterials used to conduct the mentioned studies were also produced through the FFF approach. The metamaterials behavior of interest was achieved by designing and fabricating two structures that were coupled, being suggested that the properties of the coupled structures have potential for the development of applications in the biomechanics field, since they are able to exhibit mechanical and position changes as a function of the stress applied to the material.

Other studies were carried out looking for bi-stable switching by changing the unitary cell's stiffness, considering structures associated with origami paper-folding traditional techniques. Therefore, if a specific response is requested, the need mechanical properties to accomplish such response can be tuned recurring to a suitable design of a multiple cell stacked sequence. To achieve this goal, the SLS technique was used to produce a metamaterial based on a thermoplastic [43]. Those structures with the ability of switching between stable states could have potential applications in the soft robotics field and in building morphing structures [44].

It was also reported that a Multi Photon Lithography (MPL) technique was used to produce metamaterials based on small unitary cells characterized by the ability of snapping between states [45]. The obtained structure exhibited properties concerned with its dynamic mechanical operation, in terms of stiffening and softening mechanisms of deformation. This study demonstrates that in structures under compression included in a network that incorporates other structures in continuous stress, compressed elements don't have necessarily to be in contact with each other.

Furthermore, the fabrication of bi-stable metamaterials with twisting and rotational capabilities was recently reported, by using inkjet printing technology [46]. The followed design and fabrication approaches have the great advantage of avoiding the need for post assembly, by placing specific joints to build the mentioned devices in an AM single procedure, without changing the expected mechanical properties.

Considering what was mentioned above, in the fabrication of the unitary compliant bi-stable structure developed and pointed out in this thesis, as well as in the fabrication of the larger cellular compliant

bi-stable structure developed based on the unitary one previously mentioned as a unitary building block, the FFF approach was adopted.

2.2.3 Fused Filament Fabrication

The process, which was already mentioned above, where thermoplastic filaments are heated and used for a layered printing of a structure is called Fused Filament Fabrication (FFF) and it is an AM process. Such fabrication process is also known as Fused Deposition Modeling (with the trademarked acronym FDM) and, it was used to fabricate the compliant structures described in Section 4. This process is used for the fabrication of 3D printed pieces through a layered deposition of thermoplastic filaments onto a 3D printer's printing bed [49]. This technique is based on the melting and extrusion of a thermoplastic filament and subsequent layered deposition of the filament in order to form the 3D printed object [50]. The thermoplastic filament is deposited through a heated nozzle and the resulting fiber orientation is defined by the flow in the nozzle's orifice. In most FFF 3D printing machines, the thermoplastic filament comes in the form of a spool, as the one used during the studies conducted to write this thesis.

During the extrusion process, the thermoplastic filament is introduced into a liquefier due to the rollers mechanical pressure, melting afterwards and being then extruded by the nozzle of the 3D printer. Then, when already in the printing bed, the cooled liquid material starts to solidify, transitioning from a viscous fluid to a viscoelastic solid, being part of one the printed layers. Usually, the extruder consists of a head that has the ability to perform movements in three directions (x, y, and z), depositing one layer of the thermoplastic material at a time and afterwards performing a vertical adjustment before the new layer deposition begins.

The FFF approach is known as a solution characterized by its lower costs when compared with other 3D printing approaches, even considering the running costs and the needed initial investment. This process also is considered a fabrication process that is easy to use and understand, being ideal for rapid devices prototyping. Nowadays, it is a fabrication process widely used in higher education institutions, namely in the new materials research centers, with the aim to drive innovation. It has been proven to be accurate, reliable, and allowing robust devices production [49].

2.2.4 Polylactic Acid

In the current work, compliant structures have been fabricated using Polylactic Acid (PLA), which is a common thermoplastic material for 3D printing purposes. PLA is a very brittle, biodegradable, and recyclable polyester material that is made recurring to all types of waste (agricultural residues, organic municipal solid wastes, paper, food waste, green waste, etc.). Hence, such a thermoplastic material is cost-effective, widely diffused, and easy to print. Some applications of this material rely on the food packaging industry, surgical and medical fields, textiles, and more recently in the field of engineering [47].

PLA is originated by synthesis of lactic acid and it's mechanical and physical properties are somewhat comparable to some existing petroleum-based polymers. Furthermore, it has been observed by performing mechanical tests that 3D printing with recycled PLA is a viable option when compared to virgin PLA [48].

PLA thermoplastic materials can be achieved as an amorphous glassy polymer, a semi-crystalline or a highly crystalline polymer, characterized by a melting temperature between 130 and 180 °C, and a Young's modulus ranging from 2.7 to 16 GPa. It can be obtained heat-resistant PLA thermoplastic materials with the capability to support temperatures until 110 °C. As far as the basic PLA thermoplastic materials mechanical properties are concerned, it has been observed that they stay between the mechanical characteristics of polystyrene and polyethylene terephthalate (PET) materials.

METHODOLOGY

The basis of this work is to design and 3D print a compliant bi-stable metamaterial mechanism. For the structure's design, the methodology described in the work of Song *et al.* was followed, in which a compliant mechanism with an actuated mass and a set of flexible actuators was designed [1]. The fact that this kind of mechanism does not need electrical power to work is the key point that motivates this research, so that there is a need to focus on how to correctly optimize the design for the structure to perform the desired task. Another design benefit that comes along with this study is having the lowest possible energy dissipation in the system.

Following the completion of the first bi-stable flexure mechanism, it can be used as the building block for a larger logic gate mechanism. This is possible to do by linking all the rigid body parts through bi-stable flexures. The motions resulting from this type of structure can then be used to represent the basic digital logic operations. The logic values can be represented by two different stable equilibrium states of the bi-stable mechanism. The bi-stable working principle is since loading its side will result in snapping its center part to one of the stable equilibrium states. In a mechanical logic gate, compliant connectors are used to connect the mechanical bits aiming the transmission of the logic states, 0 or 1, between the mechanical bits. Once a mechanical bit changes its logic value to other state, on one side of a connector, the corresponding kinetic energy is stored as elastic potential energy, which will be passed to the mechanical bit located at the other side of the connector and, consequently, the input force only needs to surpass one mechanical bit resistance and not the overall considered connect array.

3.1 Compliant Mechanism Structure Design and Testing

The metamaterial structure was fabricated through 3D printing. The design was done in the CAD software Fusion 360, starting by the design of the switching mechanism unit cell to use as a building block, followed by the design of a two-cell switching mechanism and after that, the assembly of a larger, fully compliant multicell switching mechanism. Following the completion of the three structures, they were exported as .stl files. For the slicing, the free software Ultimaker Cura, compatible with the Ultimaker 3 printer, was used. After slicing, .gcode files were exported for the printer. Then, through FFF, the structures were fabricated. Some parameters to consider while using the slicing software were the layer height and the infill density. The chosen parameters for all structures were 0.15 mm of layer height and 100% infill density, for the structure to be stronger. Concerning the layer height, higher values result in faster prints in lower resolution, and lower values result in slower prints in higher resolution.

As said before, the material used for printing was PLA, after an unsuccessful attempt to use Thermoplastic Polyurethane (TPU), shown in Figure 3.1, since the material did not provide the necessary stiffness for the structure to perform its switching function.



Figure 3.1 — Two four-cell TPU structures.

For the mechanical characterization, compression tests were performed on a Shimadzu AG-50kN G universal testing machine, with a compression speed of 1 mm/s as shown in Figure 3.2, resulting in a compression curve (Force vs. Stroke). In the conducted tests, the testing machine was limited to a compressive force of 1 kN, since the load cell was of 50 kN, being the results obtained out of the load cell error.

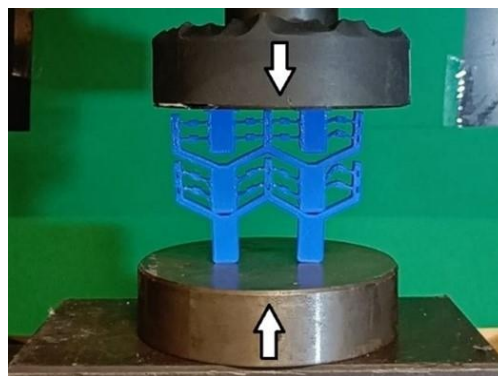


Figure 3.2 — Compression essay on a four-cell switching mechanism.

During the compression tests performed, all structures were compressed between two moving platens. Incorporated in the test machine, there is a load cell and a strain gauge, which are used to measure load (kN) and stroke (mm), respectively. The main goal of the tests was for the structures perform their switching tasks. This effect is expected to be observed because of the optimized load-bearing design of the structures.

It is also important to state that material compression testing is divisible into two forms, which depends on the speed of the test – static and dynamic modes. For the static testing, the machine should have a speed rate below 1 mm per minute, while for the dynamic testing, it should have a speed higher

than 10 mm per minute. The conducted tests fall into the static mode. Also, the static mode can be subdivided into two different categories – axial and plane strain compression testing – from which the performed tests can be categorized as axial compression tests, since the force was only applied on a vertical axis, along y-direction. The obtained results will be the peak force and the stiffness of the structures.

After the compression tests, it is expected that the structures can recuperate to their original position due to the switching mechanism. Therefore, depending on the engineered structure, one can conclude that metamaterials can present position-changing capabilities. For this to be a feasible feature of the mechanisms, some changes were made along the work. Most of these changes were concerned with the orientation and the thickness, both parameters altered in Fusion 360. Also, by adding more building blocks to the structure, a metamaterial able to achieve more advanced position changes can be created, but by doing so, one starts to limit the metamaterial's elasticity, producing inconvenient resistance in the direction of the desired deformations. To solve these problems, the successful optimization of the design was key, so that the structures' stiffness would not affect much of the flexibility. Thus, compliant multicell bi-stable structures that can perform predefined switching tasks without deformation can be manufactured.

CASE STUDIES

The current work deals with the development and fabrication of compliant bi-stable switching mechanisms. As said in the latter chapter, the CAD design, which was based on a previous work [1], was performed with the Fusion 360 software, starting by sketching a single switching mechanism cell, as shown in Figure 4.1, and extruding it, as shown in Figure 4.2. Then, recurring to Cura, slicing was performed, as portrayed in Figure 4.3. After testing and optimizing the design of the single cell switching mechanism and using it as a building block, larger fully compliant multicell switching metamaterial mechanisms as depicted in Figure 4.4 and Figure 4.5 were designed and fabricated. All structures were extruded with a thickness of 7.5 mm and with an angle of 115° between the arms and the frame.

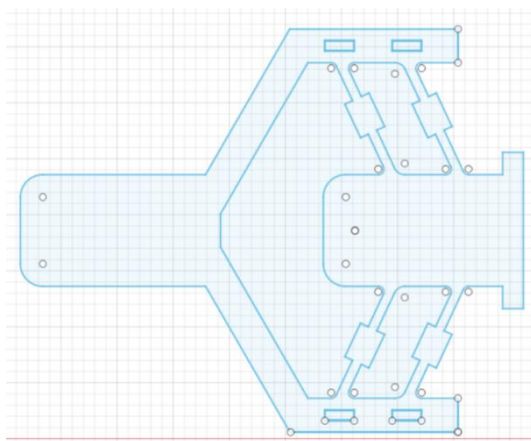


Figure 4.1 — Sketch of the single cell switching mechanism (Fusion 360).

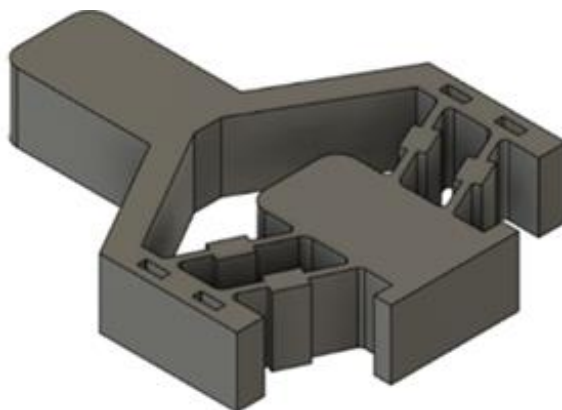


Figure 4.2 — Single cell switching mechanism (Fusion 360).

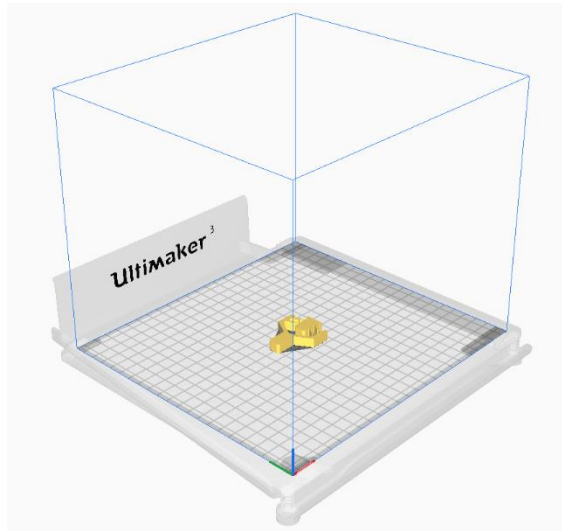


Figure 4.3 — 3D printing overview of the single cell mechanism (Fusion 360).

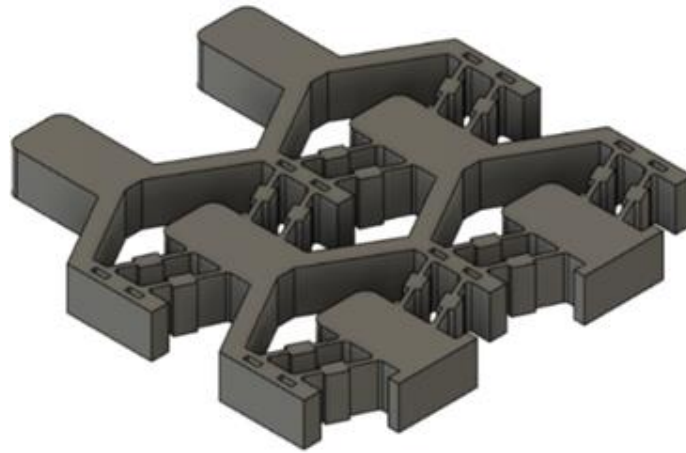


Figure 4.4 — Four-cell switching mechanism (Fusion 360).

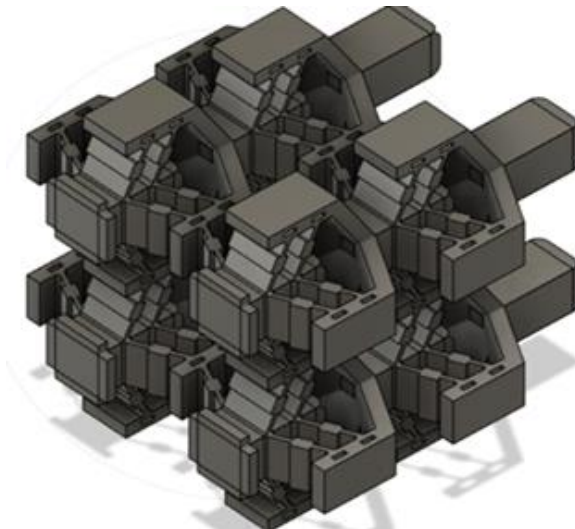


Figure 4.5 — Multicell switching mechanism (Fusion 360).

The mechanical characterization of the structures depicted above was based on compression tests, being expected that the structures are able to recuperate their original position, by reversing the switching mechanism. For this to be a possible and a feasible feature of the mechanisms, some changes had to be put into action during the undertaken studies. Most of these changes were based on arm orientation and thickness. For example, changing the angle between the arms and the frame from 110° to 115° , as depicted in Figure 4.6. This change had to be put into action, since the mechanism with a 110° angle broke under compression testing, leading to invalid results. To overcome the problems related with the addition of more building blocks to the unitary structure, it was tried to optimize the design of the mechanisms through a trial-and-error procedure, so that the structure's stiffness would not seriously hinder the desired flexibility. All compression tests took around 10 minutes to conduct, and it was possible to obtain compressive curves for the structures in all of them.

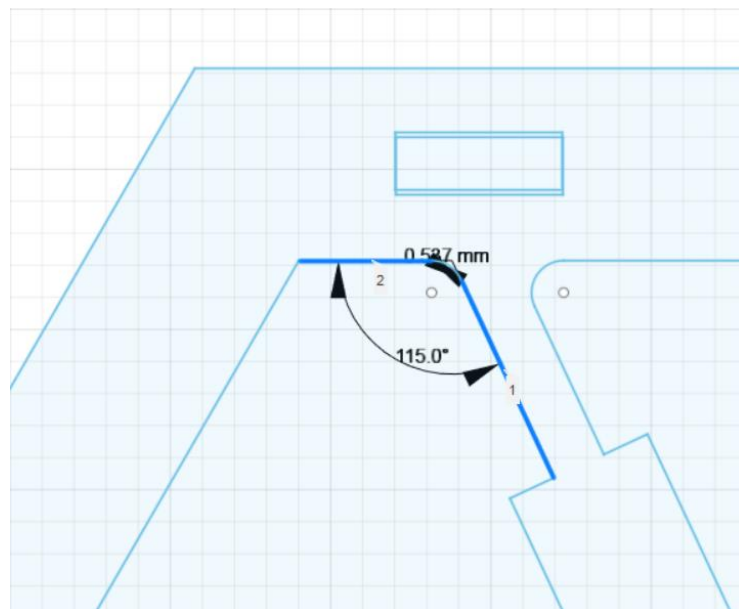


Figure 4.6 — Established angle between the arms and the frame (Fusion 360).

To compare the obtained results with the ones reported in the existing literature, in the next figure, the expected theoretical compression curve for a similar CM is shown, allowing for a better understanding on how the structure reacts to stress and if it is working accordingly to the needed requirements. The obtained compression curves should be somewhat close to the one presented in Figure 4.7, being possible to determine some parameters, such as peak force and stiffness, as well as observing the switching behavior of the structures. By analyzing Figure 4.7, it is possible to conclude that there are three points of the compression curve that have null force: the first one marks the first stable position; the second one represents a point of unstable equilibrium; and the third one marks the second stable position, meaning that the test went accordingly to the expectations by exhibiting the switching behavior of the mechanism.

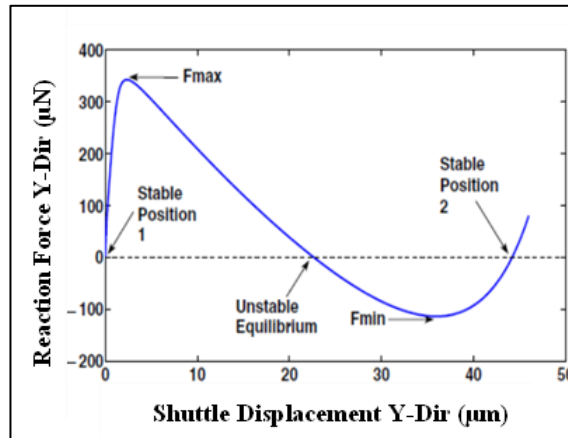


Figure 4.7 — Experimental compression test results done on Cherry *et al.*'s switching mechanism [51].

4.1 Single Cell Switching Mechanism

Figure 4.8 illustrates the manufactured single cell switching mechanism, corresponding to the designed depicted in Figure 4.2. The results obtained after being performed the corresponding mechanical compression test, representing the inherent Force vs. Displacement behavior, are plotted in Figure 4.9.

The results obtained from this test were a stiffness of $2.89E-5$ kN/mm, and a peak force of 0.09 kN, corresponding to a displacement of 3.7 mm. Observing this compression curve, it is far from the ideal behavior depicted in Figure 4.7, but it still bears some resemblances, which will be addressed in the critical analysis ahead.



Figure 4.8 — Single cell switching mechanism (after printing).

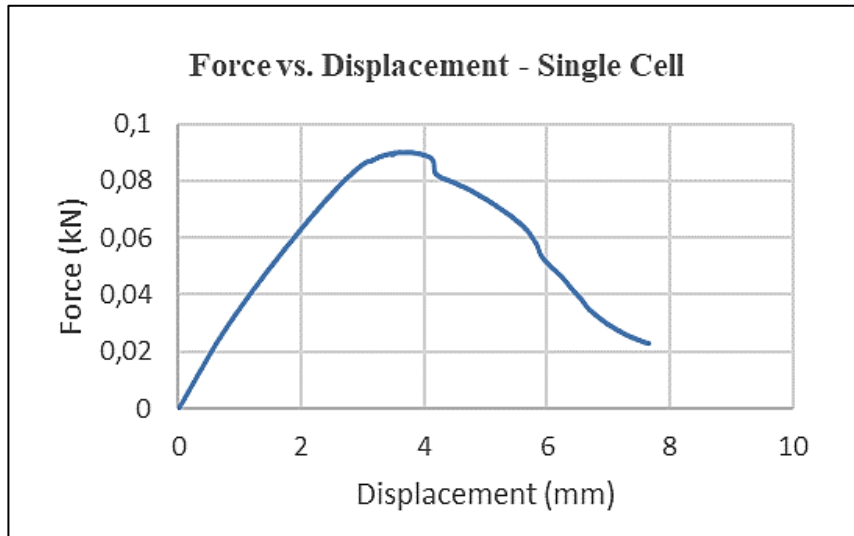


Figure 4.9 — Compression curve of the single cell switching mechanism.

Considering the reviewed literature, the plot above corresponds to what was expected. The plot starts at the point (0;0), representing one of the two points of equilibrium. It is no coincidence that, as explained before, the structure is designed in one of the two possible equilibrium positions, which means that no input force (0 N) is needed to maintain the initial configuration of the mechanism. Then the plot continues with a first linear section, where the stiffness is calculated by interpolation, to the point of maximum force (90 N) which represents the force that must be applied to move from the first position to the second stable position. The plot for the single cell switching mechanism shows a decrease in force after the point of the peak force. This decrease should ideally reach 0, which represents a point of unstable equilibrium, meaning that again no force would be required to maintain the mechanism's unstable state. However, the test was interrupted when the actuated mass came into direct contact with the frame, not allowing to progress any further. At this point, the mechanism needs an opposite force of the one applied during the compression test, so that it can recuperate its initial configuration. Ideally, the force-displacement behavior should be symmetric of the one shown in Figure 4.9. At the end of the test, when trying to apply a force in the opposite direction, it was possible to revert the mechanism back to its original equilibrium position. Since the switching performance shown by the single cell switching mechanism was quite what was predicted, it was used as the building block for the next two structures, presented in the following two subsections, starting by a four-cell switching mechanism and after a multicell switching mechanism.

4.2 Four-Cell Switching Mechanism

As for what concerns the single cell switching mechanism presented in the previous subsection, the sketched four-cell switching mechanism, which is depicted in Figure 4.10, was firstly extruded as shown in Figure 4.4, then manufactured as described above and, the device obtained is illustrated in Figure 4.12.

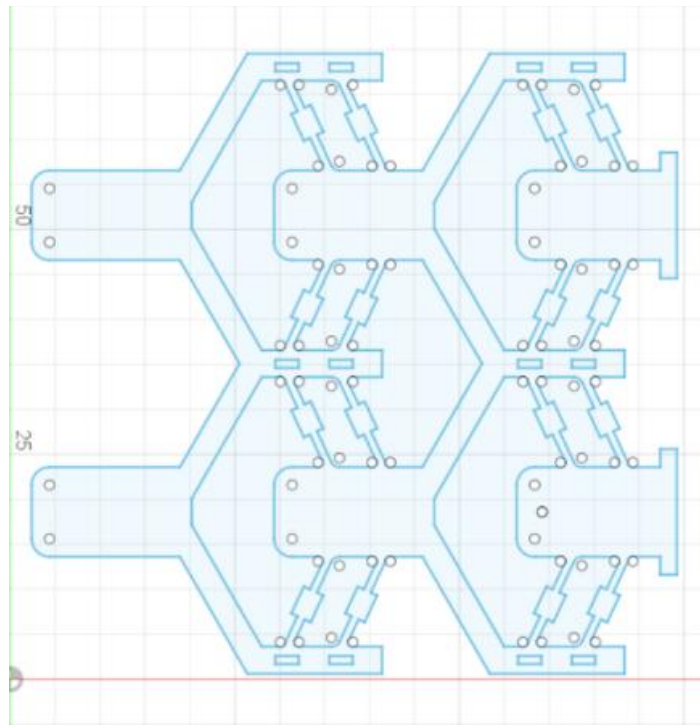


Figure 4.10 — Sketch of the four-cell switching mechanism (Fusion 360).

After the extrusion of the structure, slicing was done recurring to Cura, as portrayed in Figure 4.11.

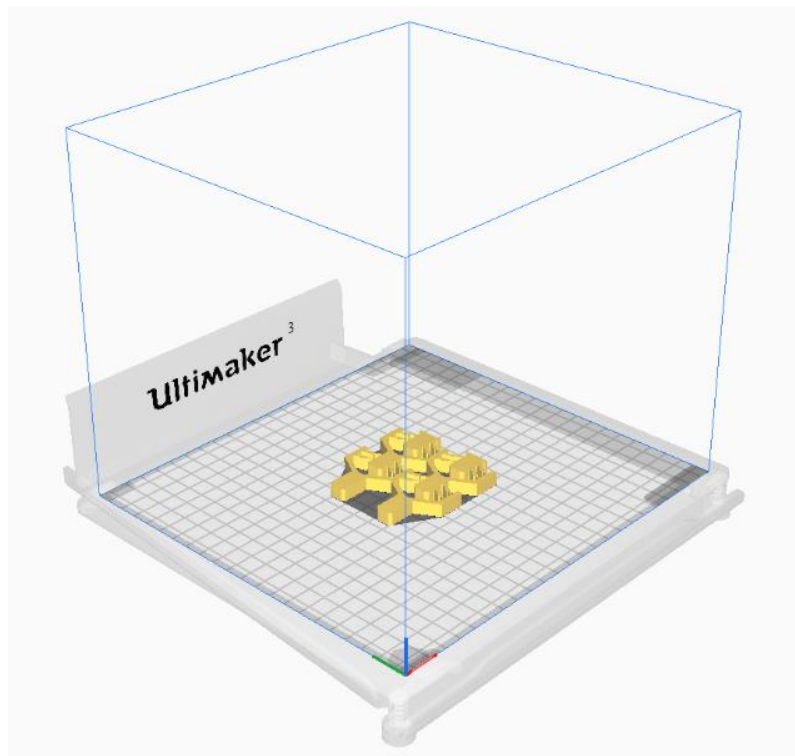


Figure 4.11 — 3D printing overview of the four-cell switching mechanism (Cura).

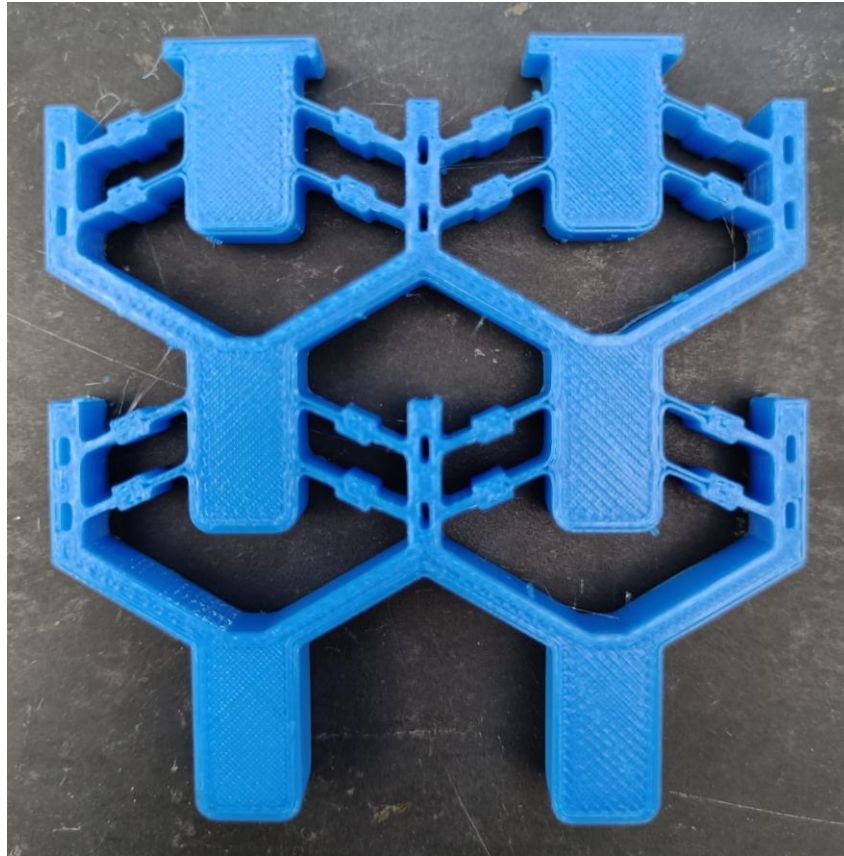


Figure 4.12 — Four-cell switching mechanism (after printing).

The results obtained from this test need to be divided into two different parts, since the two bottom cells switched firstly, and sometime later, the two top cells switched, as portrayed by the plot in Figure 4.13. For the first part of the plot, the interpolated stiffness is $3.38\text{E-}5$ kN/mm, and the peak force is 0.13 kN, corresponding to a displacement of 5.35 mm, which is already higher than the registered displacement for the single cell's peak force point. For the second part of the plot, the interpolated stiffness is $4.90\text{E-}5$ kN/mm, and the peak force is also 0.13 kN, corresponding to a displacement of 11.5 mm. The plot for the four-cell switching mechanism shows a decrease in force after the first point of peak force (130 N), which is almost 1.5 times higher than the force required for the single cell mechanism. Also, this point represents the switching of the bottom two cells. Later on, the force started to increase again, reaching another point of peak force (130 N), the same force as the first peak point, followed by another decrease. The second point of peak force represents the switching of the top two cells. The peak force increase was expected according to the literature, since the addition of three more unitary structures to the single cell one led to a decrease in elasticity, creating resistance and hampering the switching performance of the mechanism. Also, according to the previously interpolated stiffnesses, a decrease in the stiffness of the mechanism can be observed after the switching of the bottom two cells. At the end of the test, when trying to apply a force in the opposite direction of the one applied during the compression test, it was possible to revert the mechanism back to its original equilibrium position, as expected.

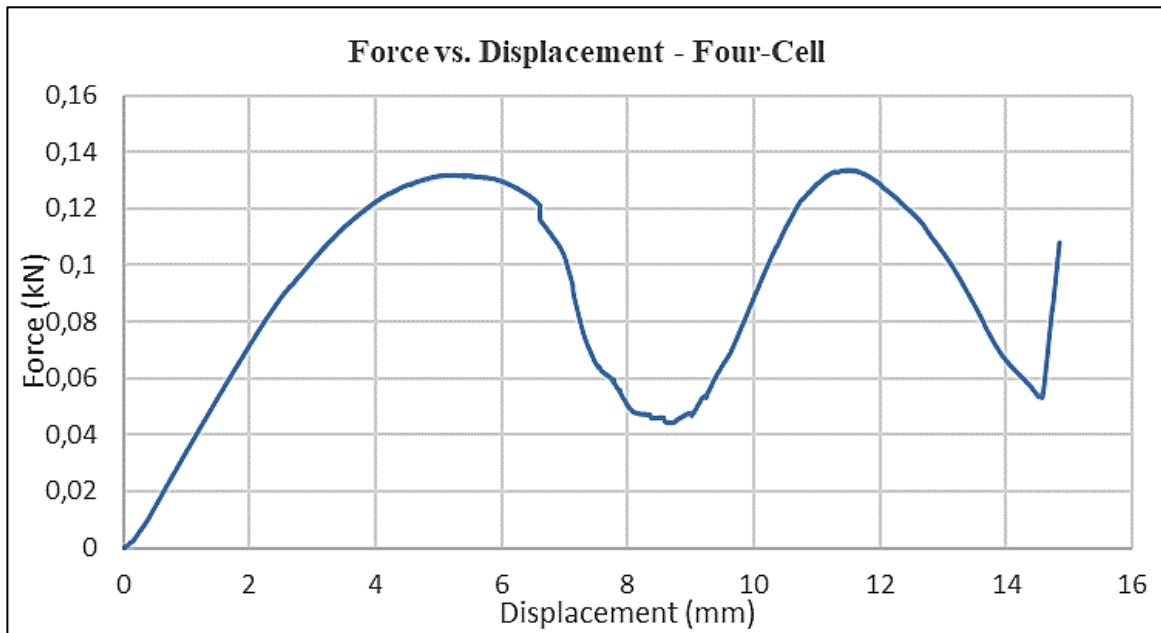


Figure 4.13 — Compression curve of the four-cell switching mechanism.

4.3 Multicell Switching Mechanism

As previously mentioned, the multicell switching mechanism was designed through the integration of several single cell switching mechanisms (a total of 8), recurring to the sketch of the four-cell switching mechanism, as depicted in Figure 4.5, sliced, as portrayed in Figure 4.14, manufactured, and the achieved device is shown in Figure 4.15.

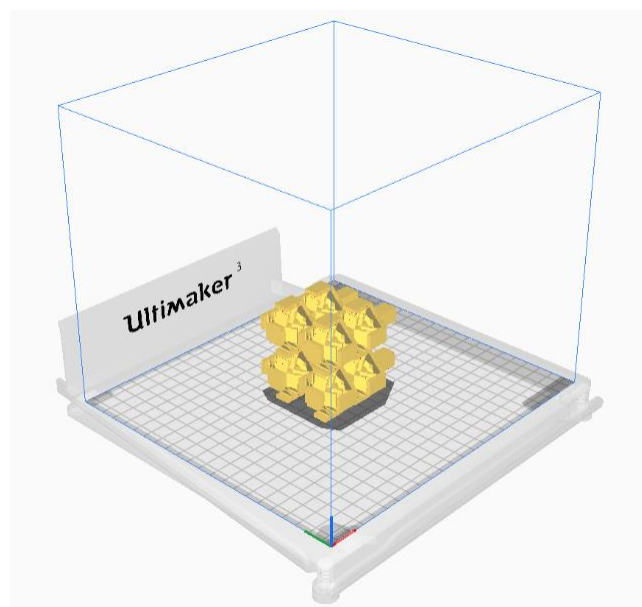


Figure 4.14 — 3D printing overview of the multicell switching mechanism (Cura).

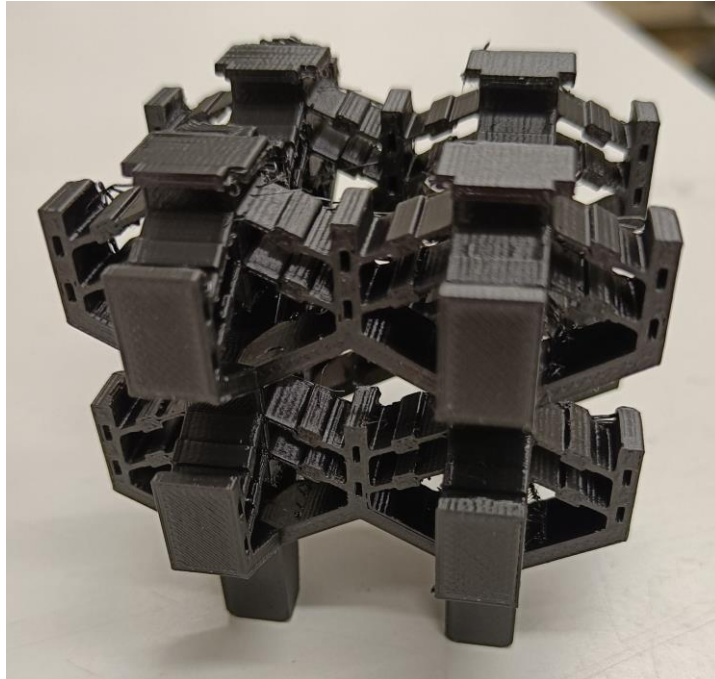


Figure 4.15 — Multicell switching mechanism (after printing).

According to the literature, the multicell structure should be the one presenting higher peak force values, since it is the one that incorporates more single cell mechanisms. The corresponding Force vs. Displacement behavior plotted in Figure 4.16, was obtained with the results acquired during the performed mechanical compression test, following the procedure mentioned to the previous devices presented in the last two subsections and the corresponding critical analysis will be presented below.

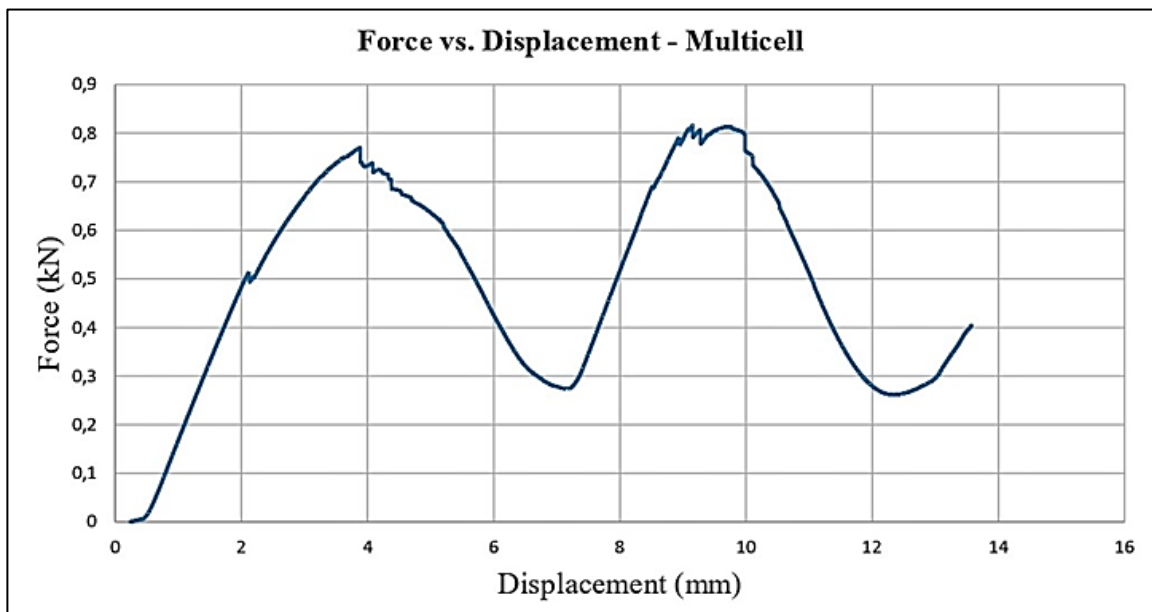


Figure 4.16 — Compression curve of the multicell switching mechanism.

The results obtained from this test also need to be divided into two different parts, since the four top cells switched firstly, and sometime later, the four bottom cells switched, as portrayed by the plot in Figure 4.10. For the first part of the plot, the interpolated stiffness is 0.32 kN/mm, and the peak force is 0.75 kN, corresponding to a displacement of 3.9 mm, which is close to the one registered for the single cell's peak point. For the second part of the plot, the interpolated stiffness is 0.34 kN/mm, and the peak force is 0.81 kN, corresponding to a displacement of 9.75 mm. The plot for the multicell switching mechanism shows a decrease in force after the first point of peak force (750 N), more than 8 times higher than for the single cell mechanism, and more than 5.5 times higher than for the four-cell mechanism. This can be explained due to the increased registered stiffness of this structure compared to the previous two. Also, note that this point only represents the switching of the top four cells. Later on, the force started to increase again, reaching an even higher point of peak force (810 N), followed by another decrease. The second point of peak force represents the switching of the bottom four cells, meaning that an even higher force was needed after the switching of top four cells, since the top four cells were being pressed onto the frame of the structure, resulting in the additional force that was measured for the bottom four cells switching. At the end of the test, when trying to apply a force in the opposite direction of the one applied during the compression test, it was possible to revert the mechanism back to its original equilibrium position.

Afterwards, repetitive solicitation tests were performed on all of the structures, where one of the actuator arms of the single cell mechanism broke after 29 full switches, one of the actuator arms of the four-cell mechanism broke after 23 full switches, and one of the actuator arms of the multicell mechanism broke after 18 full switches. This shows that with a higher complexity, and having more actuator arms, the probability for an arm breakage increases.

CONCLUSIONS AND FUTURE PERSPECTIVES

The results obtained with the design and fabrication of compliant bi-stable structures demonstrate that using 3D printing, it is possible to obtain structures able to perform mechanical functions by switching between two alternate states. The switching behavior under compressive stress, and subsequent position recovery of the structures, meaning that they do not undergo permanent deformation in the process, were observed.

A novel unitary multicell compliant bi-stable structure was designed and fabricated and was used as a building block to successfully build two larger cellular compliant bi-stable metamaterial arrays.

Conducted compression tests led to a better understanding of the structures' stiffness and maximum force needed to perform the switching function. The multicell structure proved to be the stiffest and the one that required higher compressive force to perform its function. The conducted compressive tests were also important to check if the position recovery of the structures was possible to achieve, which was observed in all of them. Also, from the conducted repetitive solicitation tests, further studies are needed in order to improve the device's reliability.

The successful results obtained foster the potential application of the structures developed in Boolean computation based on mechanical forces and displacements without using electricity, being the multicell structure the one capable of representing more complex Boolean functions.

Regarding the future, despite showing clear advantages when talking about design, portability, and cost; CMs face a big problem which is the nature of the printing material, making their usage limited. To improve the repeatability factor, one can think of combining compliant and rigid designs, or even different materials, allowing for the maximization of the advantages of the design principles. Also, when the repeatability problem is solved, larger and miniaturized multicell structures could be printed, opening new paths on how we can store more data recurring only to mechanical displacements.

BIBLIOGRAPHY

- [1] Song, Y., *et al.* (2019), "Additively manufacturable micro-mechanical logic gates". *Nature Communications*, vol. 10, article number 882, doi: 10.1038/s41467-019-08678-0.
- [2] Xu, X., *et al.* (2019). "Double negative-index ceramic aerogels for thermal superinsulation". *Science*, 363 (6428), pp. 723–727, doi: 10.1126/science.aav7304.
- [3] Surjadi, J. U., *et al.* (2019). "Mechanical metamaterials and their engineering applications". *Advanced Engineering Materials*, vol. 21, no. 3, 1800864, pp. 1-37, doi: 10.1002/adem.201800864.
- [4] Ren, C., Yang, D. and Qin, H. (2018). "Mechanical performance of multidirectional buckling based negative stiffness metamaterials: an analytical and numerical study". *Materials*, vol. 11, no. 7, 1078, doi: 10.3390/ma11071078.
- [5] Lei, M., *et al.* (2019). "3D printing of auxetic metamaterials with digitally reprogrammable shape". *ACS Applied Materials & Interfaces*, vol. 11, no. 25, pp. 22768–22776, doi: 10.1021/acsami.9b06081.
- [6] Jensen, J. S. (2003). "Phononic band gaps and vibrations in one- and two-dimensional mass–spring structures". *Journal of Sound and Vibration*, vol. 266, no. 5, pp. 1053–1078, doi: 10.1016/S0022-460X(02)01629-2.
- [7] Kafesaki, M., Sigalas, M. M. and García, N. (2000). "Frequency modulation in the transmittivity of wave guides in elastic-wave band-gap materials". *Physical Review Letters*, vol. 85, no. 19, pp. 4044–4047, doi: 10.1103/PhysRevLett.85.4044.
- [8] Greer, J. R. and Deshpande, V. S. (2019). "Three-dimensional architected materials and structures: Design, fabrication, and mechanical behavior". *MRS Bulletin*, vol. 44, no. 10, pp. 750–757, doi: 10.1557/mrs.2019.232.
- [9] Kumar, P., Schmidleithner, C., Larsen, N. B. and Sigmund, O. (2021). "Topology optimization and 3D printing of large deformation compliant mechanisms for straining biological tissues". *Structural and Multidisciplinary Optimization*, vol. 63, pp. 1351–1366, doi: 10.1007/s00158-020-02764-4.
- [10] Magleby, S. P. (2013). "Using the Handbook to Design Devices". In *Handbook of Compliant Mechanisms*, edited by Larry L. *et al.*, pp. 15-25, doi: 10.1002/9781118516485.ch230.

- [11] Shaw, L. A., *et al.* (2019). "Computationally efficient design of directionally compliant metamaterials". *Nature Communications*, vol. 10, article number 291, doi: 10.1038/s41467-018-08049-1.
- [12] Kota, S., *et al.* (2001). "Design of Compliant Mechanisms: Applications to MEMS". *Analog Integrated Circuits and Signal Processing*, vol. 29, pp. 7–15, doi: 10.1023/A:1011265810471.
- [13] Lobontiu, N. (2003). *Compliant mechanisms: design of flexure hinges*. CRC Press LLC, Florida, United States of America, ISBN: 0-8493-1367-8.
- [14] Liashenko, I., Rosell-Llompart, J. and Cabot, A. (2020). "Ultrafast 3D printing with submicrometer features using electrostatic jet deflection". *Nature Communications*, vol. 11, article number 753, doi: 10.1038/s41467-020-14557-w.
- [15] Lee, J. H., Singer, J. P. and Thomas, E.L. (2012). "Micro-/nanostructured mechanical metamaterials". *Advanced Materials*, vol. 24, pp. 4782–4810, doi: 10.1002/adma.201201644.
- [16] Zadpoor, A. A. (2016). "Mechanical meta-materials". *Materials Horizons*, vol. 3, pp. 371–381, doi: 10.1039/c6mh00065g.
- [17] Lee, W., Kang, D. Y., Song J., Moon, J. H. and Kim, D. (2016). "Controlled unusual stiffness of mechanical metamaterials". *Scientific Reports*, vol. 6, article number: 20312, doi: 10.1038/srep20312.
- [18] Zheng, X., *et al.* (2014). "Ultralight, ultrastiff mechanical metamaterials". *Science*, vol. 344, no. 6190, pp. 1373–1377, doi: 10.1126/science.1252291.
- [19] Bückmann, T., *et al.* (2014). "An elasto-mechanical unfeelability cloak made of pentamode metamaterials". *Nature Communications*, vol. 5, article number: 4130, doi: 10.1038/ncomms5130.
- [20] Hengsbach, S. and Lantada, A. D. (2014). "Direct laser writing of auxetic structures: present capabilities and challenges". *Smart Materials and Structures*, vol. 23, article number: 085033, doi: 10.1088/0964-1726/23/8/085033.
- [21] Kolken, H. M. A. and Zadpoor, A. A. (2017). "Auxetic mechanical metamaterials". *RSC Advances*, vol. 7, pp. 5111–5129, doi: 10.1039/c6ra27333e.
- [22] Frenzel, T., Kadic, M. and Wegener, M. (2017). "Three-dimensional mechanical metamaterials with a twist". *Science*, vol. 358, no. 6366, pp. 1072–1074, doi: 10.1126/science.aao4640.
- [23] Kadic, M., *et al.* (2014). "Pentamode metamaterials with independently tailored bulk modulus and mass density". *Phys. Review Applied*, vol. 2, art. no: 054007, doi: 10.1103/PhysRevApplied.2.054007.
- [24] Hedayati, R., Leeflang, A. M. and Zadpoor, A. A. (2017). "Additively manufactured metallic pentamode meta-materials". *Applied Physics Letters*, vol. 110, no. 9, article number: 091905, doi: 10.1063/1.4977561.
- [25] Mohsenizadeh, M., Gasbarri, F., Munther, M., Beheshti, A. and Davami, K. (2018). "Additively-manufactured lightweight metamaterials for energy absorption". *Materials & Design*, vol.139, pp. 521–530, doi: 10.1016/j.matdes.2017.11.037.

- [26] dell'Isola, F., *et al.* (2019). "Pantographic Metamaterials: an Example of Mathematically Driven Design and of its Technological Challenges". *Continuum Mechanics and Thermodynamics*, vol. 31, pp. 851–884, doi: 10.1007/s00161-018-0689-8.
- [27] Jacobsen, A. J., *et al.* (2010). "Interconnected self-propagating photopolymer waveguides: an alternative to stereolithography for rapid formation of lattice-based open-cellular materials". *Proc. of 2010 International Solid Freeform Fabrication Symposium*, pp. 846–853, doi: 10.26153/tsw/15249.
- [28] Bauer, J., Schroer, A., Schwaiger, R. and Kraft, O. (2016). "Approaching theoretical strength in glassy carbon nanolattices". *Nature Materials*, vol. 15, pp. 438–443, doi: 10.1038/nmat4561.
- [29] Torrents, A., *et al.* (2012). "Characterization of nickel-based microlattice materials with structural hierarchy from the nanometer to the millimeter scale." *Acta Materialia*, vol. 60, no. 8, pp. 3511–3523, doi: 10.1016/j.actamat.2012.03.007.
- [30] Han, S. C., Lee, J. W. and Kang, K. (2015). "A new type of low density material: shellular". *Advanced Materials*, vol. 27, pp. 5506–5511, doi: 10.1002/adma.201501546.
- [31] Mieszala, M., *et al.* (2017). "Micromechanics of amorphous Metal/Polymer hybrid structures with 3D cellular architectures: size effects, buckling behavior, and energy absorption capability". *Small*, vol. 13, no. 8, article number:1602514, doi: 10.1002/sml.201602514.
- [32] Montemayor, L. C. and Greer, J. R. (2015). "Mechanical response of hollow metallic nanolattices: combining structural and material size effects". *Journal of Applied Mechanics*, vol. 82, no. 7, article number: 071012, doi: 10.1115/1.4030361.
- [33] Meza, L. R., Das, S. and Greer, J. R. (2014). "Strong, lightweight, and recoverable three-dimensional ceramic nanolattices". *Science*, vol. 345, no. 6202, pp. 1322–1326, doi: 10.1126/science.1255908.
- [34] Bauer, J., Hengsbach, S., Tesari, I., Schwaiger, R. and Kraft, O. (2014). "High-strength cellular ceramic composites with 3D microarchitecture". *Proc. of the National Academy of Sciences of the United States of America*, vol. 111, no. 7, pp. 2453–2458, doi: 10.1073/pnas.1315147111.
- [35] Schwerdtfeger, J., *et al.* (2012). "Mechanical characterization of a periodic auxetic structure produced by SEB". *IPSS Basic Solid State Physics*, vol. 249, pp.1347–1352, doi: 10.1002/pssb.201084211.
- [36] Mark, A. G., *et al.* (2016). "Auxetic metamaterial simplifies soft robot design". *Proc. of 2016 IEEE Int. Conf. on Robotics and Automation (ICRA)*, pp. 4951–4956, doi: 10.1109/ICRA.2016.7487701.
- [37] Bauer, J., *et al.* (2017). "Nanolattices: An Emerging Class of Mechanical Metamaterials". *Advanced Materials*, vol. 29, no. 40, article number: 1701850, doi: 10.1002/adma.201701850.
- [38] Ali, M. N., Busfield, J. J. C. and Rehman, I. U. (2014). "Auxetic oesophageal stents: structure and mechanical properties". *Journal of Materials Science: Materials in Medicine*, vol. 25, pp. 527–553, doi: 10.1007/s10856-013-5067-2.

- [39] Yuan, S., Shen, F., Bai, J., Chua, C. K., Wei, J. and Zhou, K. (2017). "3D soft auxetic lattice structures fabricated by selective laser sintering: TPU powder evaluation and process optimization". *Materials & Design*, vol. 120, pp. 317–327, doi: 10.1016/j.matdes.2017.01.098.
- [40] Rafsanjani, A., Akbarzadeh, A. H. and Pasini, D. (2015). "Snapping mechanical metamaterials under tension". *Advanced Materials*, vol. 27, pp. 5931–5935, doi: 10.1002/adma.201502809.
- [41] Che, K., Yuan, C., Wu, J., Qi, H. J. and Meaud, J. (2017). "Three-dimensional-printed multistable mechanical metamaterials with a deterministic deformation sequence". *Journal of Applied Mechanics*, vol. 84, article number: 011004, doi: 10.1115/1.4034706.
- [42] Yang, H. and Ma, L. (2020). "Angle-dependent transitions between structural bistability and multistability". *Advanced Engineering Materials*, vol. 22, article number: 1900871, doi: 10.1002/adem.201900871.
- [43] Sengupta, S. and Li, S. (2018) "Harnessing the anisotropic multistability of stacked-origami mechanical metamaterials for effective modulus programming". *Journal of Intelligent Material Systems and Structures*, vol. 29, pp. 2933–2945, doi: 10.1177/1045389X18781040.
- [44] Fang, H., Li, S., Ji, H. and Wang, K. W. (2017). "Dynamics of a bistable Miura-origami structure". *Physical Review E*, vol. 95, no. 5, article number: 52211, doi: 10.1103/PhysRevE.95.052211.
- [45] Vangelatos, Z., Micheletti, A., Grigoropoulos, C. P. and Fraternali, F. (2020). "Design and testing of bistable lattices with tensegrity architecture and nanoscale features fabricated by multiphoton lithography". *Nanomaterials* 2020, vol. 10, no. 4, article number: 652, doi_ 10.3390/nano10040652.
- [46] Jeong, H. Y., *et al.* (2019). "3D printing of twisting and rotational bistable structures with tuning elements". *Scientific Reports*, vol. 9, article number: 324, doi: 10.1038/s41598-018-36936-6.
- [47] Han, J. H. (2014). *Innovations in Food Packaging*. Elsevier Academic Press, Second Edition, Food Science and Technology International Series, USA, doi: 10.1016/C2011-0-06876-X.
- [48] Anderson, I. (2017). "Mechanical Properties of Specimens 3D Printed with Virgin and Recycled Polylactic Acid". *3D Printing and Additive Manufacturing*, vol. 4, no. 2, pp. 110-115, doi: 10.1089/3dp.2016.0054.
- [49] Rebelo, H. B., *et al.* (2019). "Experimental and numerical investigation on 3D printed PLA sacrificial honeycomb cladding". *International Journal of Impact Engineering*, vol. 131, pp. 162-173, doi: 10.1016/j.ijimpeng.2019.05.013.
- [50] Santos, F. A., *et al.* (2021). "Low velocity impact response of 3D printed structures formed by cellular metamaterials and stiffening plates: PLA vs. PETg". *Composite Structures*, vol. 256, 113128, doi: 10.1016/j.compstruct.2020.113128.
- [51] Cherry, B. B., Howell, L. L. and Jensen, B. D. (2008). "Evaluating three-dimensional effects on the behavior of compliant bistable micromechanisms". *Journal of Micromechanics and Microengineering*, vol. 18, no. 9, 095001, doi: 10.1088/0960-1317/18/9/095001.



(2022)

RICARDO CALADO

ADDITIVE MANUFACTURING OF RESETTABLE-DEFORMATION BI-STABLE LATTICES BASED ON A COMPLIANT MECHANISM



<2022>

RICARDO CALADO

ADDITIVE MANUFACTURING OF RESETTABLE-DEFORMATION BI-
STABLE LATTICES BASED ON A COMPLIANT MECHANISM

